

The temperature of shock-compressed water^{a)}

G. A. Lyzenga^{b)} and Thomas J. Ahrens

California Institute of Technology, Seismological Laboratory, Pasadena, California 91125

W. J. Nellis and A. C. Mitchell

Lawrence Livermore National Laboratory, Livermore, California 94550

(Received 26 October 1981; accepted 12 March 1982)

Temperatures from 3300–5200 K were measured in liquid H₂O shocked to 50–80 GPa (500–800 kbar). A six-channel, time-resolved optical pyrometer was used to perform the measurements. Good agreement with the data is obtained by calculating the temperature with a volume-dependent Grüneisen parameter derived from double-shock data and a heat capacity at constant volume of 8.7 R per mole of H₂O.

I. INTRODUCTION

The temperature of shocked water has been measured near 2000 K by Kormer.¹ Water has been the subject of numerous other dynamic compression studies, as discussed in the previous paper.² Dynamic equation of state experiments on water are based on the Rankine–Hugoniot conservation equations which relate kinematic parameters to pressure, density, and specific internal energy in the shock state. The temperature of shocked material is generally calculated from a theoretical model^{3–5} because very few shock temperature measurements have ever been performed. On the other hand, temperature is an important thermodynamic parameter because it can provide information about the partition of internal energy. In shocked water, for example, internal energy is distributed among several degrees of freedom including kinetic energy, potential energy due to the intermolecular repulsion, molecular vibrational and rotational energy, and possibly energy absorbed by molecular ionization and electronic excitation. Theories based on statistical mechanics are currently being developed for compressed small molecules, which take these phenomena into account.^{6,7} Temperature is an explicit variable in these theories and the calculated temperature is quite sensitive to the extent to which various degrees of freedom are activated, especially in a polyatomic molecule like H₂O. Thus, temperature measurements are very important for constructing a reliable theoretical model and equation of state for water at high densities and temperatures.

Recent nonequilibrium molecular dynamics simulations⁸ and solutions of the Navier–Stokes equations⁹ both show that shock widths are of the order 1 nm or a few molecular diameters for strong shock waves in a dense simple fluid. The shock width is the distance over which the fluid changes from its initial state to a state of thermal equilibrium behind the shock front. This experiment is designed to measure the spectrum of the thermal radiation emitted by the shocked fluid behind the narrow width of the shock front.

We have developed a pyrometric method for measuring the shock temperature of optically transparent materials at the Lawrence Livermore National Laboratory two-stage, light-gas gun.^{10,11} We have applied this technique to water. These measurements were made in the range 3300–5200 K for shock pressures of 50–80 GPa (500–800 kbar). In the following paper Ree reports a quantum statistical mechanics theory for dense, high-temperature water and compares the results to the data. Above 3000 K the theory overestimates the measured temperature by ~17%. However, the theory does not include molecular ionization which is significant at the conditions achieved in these experiments.¹²

II. EXPERIMENT

The series of shock temperature experiments on H₂O was carried out employing the experimental technique and apparatus described in detail earlier.¹⁰ Liquid H₂O samples were shock compressed by the plate impact method. The Lawrence Livermore National Laboratory light-gas gun¹¹ was used to accelerate tantalum or copper plates of ~2 mm thickness to velocities between 4.9 and 6.7 km/s. In such experiments, a planar shock is transmitted from an aluminum base plate to the water sample, as shown in Fig. 1.

As the shock front moves into the water layer, electrical shorting pins mark the shock arrival and provide the necessary diagnostic triggering and fiducial pulses. The shock-compressed H₂O behind the advancing front is strongly heated, and becomes sufficiently opaque so as to emit strong thermal radiation. This visible radiation may escape in the forward direction, through the uncompressed and still transparent layer of the sample. In order to contain the liquid sample, a transparent sapphire (α -Al₂O₃) radiation window forms the rear wall of the sample chamber. Thus, thermal radiation from the shock-compressed sample can be observed remotely by the electrooptical pyrometer system described previously.¹⁰

The metallic base plate (Fig. 1) was composed of aluminum (alloy 1100) with a thickness of 2 mm. The sample cavity was constructed to allow a 3–4 mm shock propagation distance in water. The chamber was filled with high purity deionized water through the fill tubing depicted in Fig. 1 and was made free of bubbles and contaminants by repeatedly evacuating and flushing the

^{a)}Work performed under the auspices of the U. S. Department of Energy by the Lawrence Livermore National Laboratory under contract number W-7405-ENG-48.

^{b)}Present address: Jet Propulsion Laboratory, Pasadena, CA 91103.

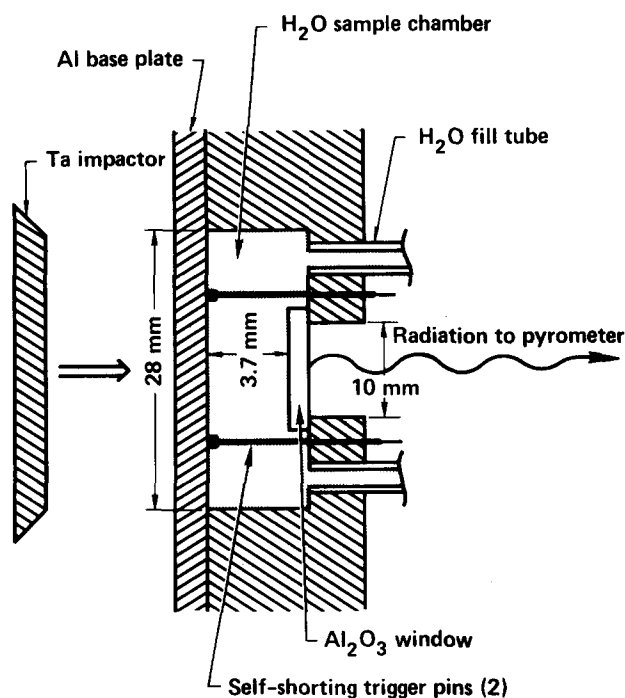


FIG. 1. Schematic cross section of the water target assembly and the impactor. On impact a shock is driven into the H_2O sample through an aluminum base plate. A sapphire window forms the rear wall of the H_2O chamber. Shorting pins provide a trigger pulse to oscilloscopes which record the pyrometer signals during the 300–400 ns propagation time of the shock through the 3.7 mm thick water sample.

cavity with pure water. A copper-constantan thermocouple was used to monitor the sample initial temperature, and thus also provide an accurate determination of the initial water density.

Figure 2 shows a typical experimental record of detected thermal radiation in the 506 nm channel at a pressure of 62 GPa. This oscillogram was obtained by a Tektronix 585 oscilloscope.¹³ Tektronix 7903 oscilloscopes were used as well. This record is qualitatively similar to those obtained in experiments with other transparent materials,¹⁴ displaying a nearly constant plateau of sample radiance during the approximately 400 ns period of shock transit. After the shock wave propagates through the H_2O layer, it encounters the sapphire window. Since sapphire has a higher shock impedance than water,¹⁵ a reflected shock of higher amplitude is driven back into the sample. This accounts for the sudden increase in observed light intensity at the instant of shock arrival at the window. The values of H_2O shock temperature reported here are computed from the first-shock plateau intensities. For the shot at highest pressure (WET3) the intensity of the plateau increases with time and represents an apparent increase in the temperature of 70 K or 1.3%. The shock temperature was obtained from the spectrum at the end of the first-shock plateau. The source of this time dependence is currently under investigation.

In all but a single case, a shock of constant amplitude was generated in the H_2O by the tantalum–aluminum driver combination. The exception is the shot at 58.5

GPa peak pressure. In this experiment, a thin (0.75 mm) copper impactor replaced the tantalum projectile, in order to observe a shock of decaying amplitude. Figure 3 shows the pyrometer output from this shot. As indicated, the unattenuated steady shock moves through the water layer during the initial 250 ns of the record. It is from this portion of the record that the spectral radiance values and shock temperature are derived. At this point in the record, the overtaking of the shock by relaxation waves from the free surface of the thin flyer is observed as an abrupt attenuation of the shock amplitude and accompanying thermal radiation. It is noteworthy that the relatively sharp break in the record indicates that the pyrometer “sees” only a short distance into the shocked region, a result which is in agreement with earlier conclusion that a sufficiently strong shock front gives rise to an essentially opaque radiating layer, in thermal equilibrium with the compressed state.

III. RESULTS

The six-channel spectral radiance data were corrected for losses at the interfaces between liquid and sapphire window and between window and vacuum by means of the Fresnel equations. The data were also corrected for the measured wavelength-dependent losses at the turning mirror¹⁶ which reflects the radiation to the pyrometer. The spectral radiance data were least squares fitted to a graybody spectrum and the temperatures T and emissivities ϵ obtained are listed in Table I. The fit parameters were chosen subject to the constraint that $\epsilon \leq 1$. The fractional standard deviations of the data from the fits are 8% or less, which is of the order of the estimated uncertainty in the measurement of the radiance in a given channel. The standard deviations of the temperature and emissivity due to random uncertainties of 10% per channel are about 40 K and 0.02,

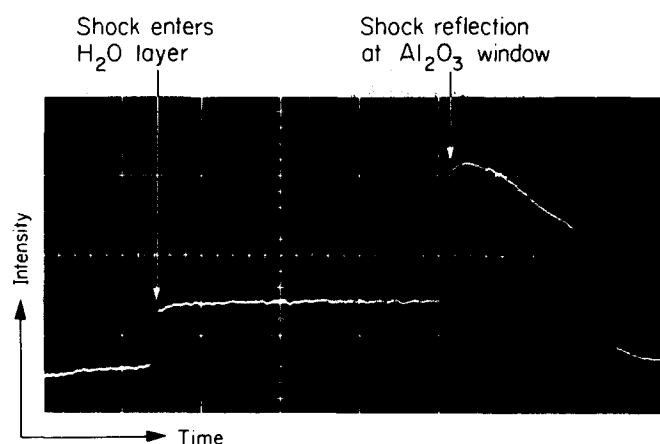


FIG. 2. Typical light intensity record from H_2O -shock-temperature experiment, shot WET4. Shock transit through water layer displays constant thermal radiation output. Shock reflection from Al_2O_3 window is accompanied by an abrupt brightness increase. Record is for H_2O shock pressure of 62 GPa and for the 506 nm channel. Horizontal time base scale is 100 ns per division, while each vertical division is approximately $3 \times 10^{12} \text{ Wm}^{-3} \text{ sr}^{-1}$.

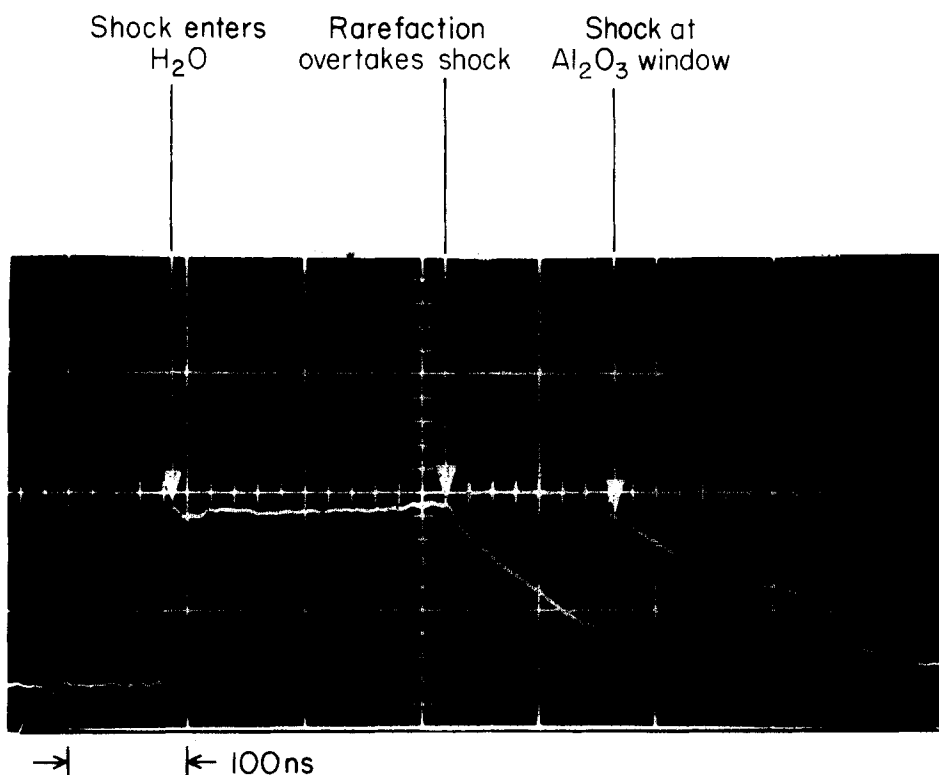


FIG. 3. Experimental record from a shock decaying from 59 GPa on shot WET5. A rarefaction overtakes and attenuates the shock wave at the indicated time. Each horizontal division is 100 ns.

respectively. However, if the emissivity is not constrained to be ≤ 1 , then three of the experiments give temperatures 100–200 K lower and emissivities 10%–20% higher. Thus, we assign absolute uncertainties of 200 K and 0.15, respectively, which are caused primarily by systematic errors in the measurements and/or data reduction process. Thus, within the accuracy of the data, shocked H_2O in the pressure range 50–80 GPa radiates as a blackbody ($\epsilon = 1$). The spectra are plotted in Fig. 4 for all the experiments.

The Hugoniot pressure–density reported in Table I were obtained from experimental measurements of impactor velocity, and previous knowledge of the Hugoniot equations of state for the target and projectile materials using the impedance matching method.¹⁷ The Hugoniots of the metals were published previously¹⁸ and are listed in Table II in terms of the linear fits to shock velocity u_s versus mass velocity u_p . The fit to the H_2O Hugoniot data² is also listed in Table II. The calculation of the release isentrope of the Al wall was described earlier.¹⁹

IV. DISCUSSION

The radiation spectrum is a continuum and shows that electrons are the source of the emitted light. Since the light is being radiated from a region close to the shock front, the electron concentration is sufficient to make the shock front opaque. However, there are not sufficient numbers of electrons present to contribute significantly to the electrical conductivity, which is dominated by ionic conduction.¹² Since electron–phonon relaxation times are of the order 10^{-14} s in good metals and less in such a very poor electrical conductor like shocked water, the resolution time of the detection system of $\sim 10^{-8}$ s is sufficiently long for the radiating electrons to come into thermal equilibrium with the shock-compressed water molecules.

In the special case, like the alkali–halides, in which the shock temperature becomes comparable to the activation energy for conduction electrons, a thin layer of free electrons near the shock front, but not in thermal

TABLE I. Shock temperatures and emissivities for water. The pressures and densities were obtained by shock impedance matching.

Shot	Impactor	U_I (km/s)	Pressure (GPa) ^a	Density (g/cm ³)	Temperature (K)	Emissivity
WET6	Ta	4.906	48.9 ± 0.9	2.26 ± 0.01	3280	0.87
WET5	Cu	6.111	58.5 ± 1.1	2.34 ± 0.01	3830	1.00
WET4	Ta	5.689	61.9 ± 1.2	2.36 ± 0.01	4090	1.00
WET2	Ta	6.2	71.0 ± 3.0	2.41 ± 0.02	4480	0.94
WET3	Ta	6.657	80.0 ± 1.8	2.47 ± 0.01	5270	1.00

^a 1 GPa = 10 kbar.

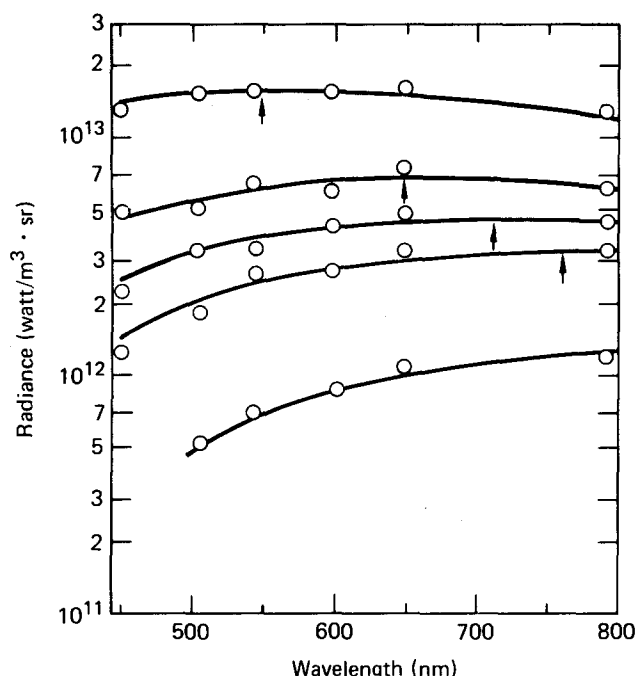


FIG. 4. Spectral radiance for all experiments. Circles are data. Solid curves are best fits using temperatures and emissivities listed in Table I. Arrows point to maxima in fitted spectra.

equilibrium with the bulk of the shocked material, can screen the thermal radiation emitted from the bulk of the shocked material. In this case the apparent temperature is significantly lower than the equilibrium temperature and saturates with increasing shock pressure.¹ No evidence for such screening occurs in these experiments because the maximum shock temperature (~ 0.5 eV) is small compared to the electronic ionization energy of the water molecule (~ 12 eV), because the measured temperatures are in reasonable agreement with the values calculated using the theoretical models discussed below, and because the measured temperatures show no indication of saturation with shock pressure.

Figure 5 shows the measured H_2O shock temperatures plotted as a function of principal Hugoniot pressure. The measured temperatures increase linearly with shock pressure. Also shown are the calculations of Rice and Walsh,³ Cowperthwaite and Shaw,⁵ and Ree,⁷ as well as the lower-pressure experimental points re-

TABLE II. Coefficients C and S , where $u_s = C + Su_p$, for the Hugoniot of Al, Cu, Ta, and H_2O used in the shock impedance matching to obtain the pressure and density of shocked H_2O .

Material	$C(\text{cm}/\mu\text{s})$	S
Al ^a	0.5386	1.339
Cu ^a	0.3933	1.500
Ta ^a	0.3293	1.307
H_2O^b	0.2393	1.333

^aReference 18.

^bReference 2.

ported by Kormer,¹ using the two wavelength black-body method. Our results are in qualitative agreement with the temperature calculations. In particular, there is no sign of breaks or discontinuities in the temperature like those which have been observed in a number of shocked solids^{1,14} and have been associated with first order phase transitions such as melting.

The curve through the data in Fig. 5 was calculated using a Grüneisen model. This model is useful when the Grüneisen parameter

$$\gamma = V \left(\frac{\partial P}{\partial E} \right)_V \quad (1)$$

is volume dependent only. This assumption is certainly not valid for H_2O for which γ is temperature dependent as well; i.e., additional degrees of freedom are excited as the temperature is increased at constant volume. However, we performed the calculations assuming that γ is dependent only on volume to estimate thermodynamic parameters of shocked water. The calculation will now be outlined.

If at a given volume, the Hugoniot pressure P_H is known as well as the state (P_r , T_r) on some reference curve, such as the compression isotherms or isentrope, then Eq. (1) allows evaluation of the internal energy difference between these states. In this case,

$$E_H - E_r = \int_{P_r}^{P_H} \frac{V}{\gamma} dP = \int_{T_r}^{T_H} C_v(V, T) dT \quad (2)$$

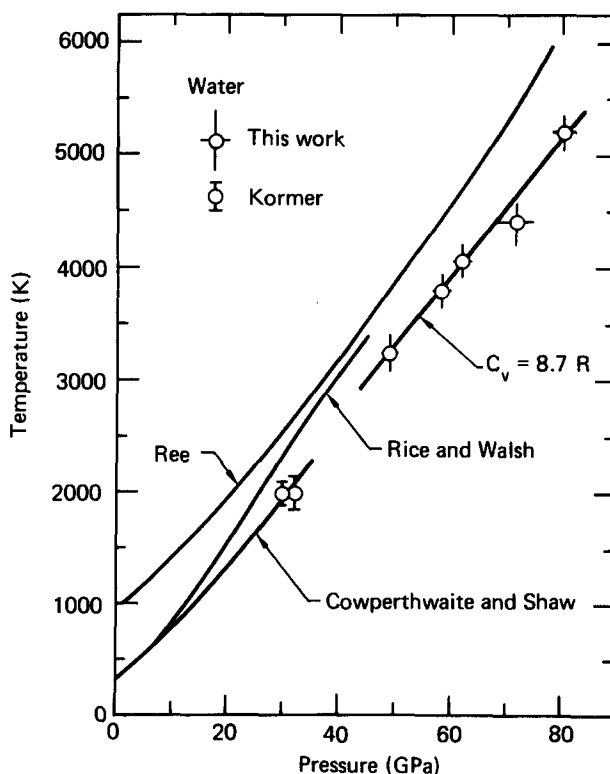


FIG. 5. H_2O shock temperature data plotted as a function of pressure. Results of the current investigation are shown with those of Kormer (Ref. 1). The line through high-pressure data was calculated by the method described in the text. Theoretical calculations are from Refs. 3, 5, and 7.

If the reference equation of state $P_r(V)$ is previously known, then it is straightforward to compute theoretical values of T_H by specifying $\gamma(V, T)$ and C_v , the specific heat at constant volume. In the majority of cases, however, the Hugoniot is the only experimentally determined curve at very high pressures, so that the reference curve must be calculated in a self-consistent manner from the Hugoniot data and the thermal model $\gamma(V, T)$. For example, when the reference curve is the compression isentrope $P_s(V)$, the energy relations lead to the differential equation for P_s ,

$$\frac{dP_s}{dV} = \frac{dP_H}{dV} + \frac{\gamma}{V} \frac{d}{dV} \left(\frac{V}{\gamma} \right) (P_H - P_s) + \frac{\gamma}{2V} \left[(V_0 - V) \frac{dP_H}{dV} - P_H - 2P_s \right]. \quad (3)$$

When, at any given V , the appropriate value of γ is assumed independent of temperature, then $P_r = P_s(V)$ can be calculated numerically, which in turn leads to the solution of Eq. (2) for the theoretical shock temperature T_H .

The Grüneisen parameter can be estimated from double-shock experiments. Figure 11 of the preceding paper summarizes γ versus density derived by this method.² The relation

$$\gamma = 0.5 + 3.27 \mu - 2.64 \mu^2, \quad (4)$$

where $\mu = (\rho/\rho_0 - 1)$ and ρ and ρ_0 are the shock density and initial density, respectively, has the correct zero-pressure value and provides a reasonable fit to the decreasing γ region at densities greater than 1.7 g/cm^3 .

Our calculations have demonstrated that substantial variations in the magnitude and volume dependence of γ have only weak effect on the calculated temperatures. In the present case, temperature calculations using a constant $\gamma = 0.9$ yielded results very similar to the case of Eq. (4), except with a larger P - T slope. For this reason, in subsequent discussion the γ description of Eq. (4) will be assumed in all calculations.

The specific heat C_v has a much greater effect in shock temperature calculations. Gurtman *et al.*,⁴ used a value of $C_v \approx 3300 \text{ J kg}^{-1} \text{ K}^{-1}$ or $7.1R$ per mol of H_2O which was derived for liquid H_2O near 2.5 GPa pressure. Using this specific heat value yields agreement with the calculations of Rice and Walsh³ but predicts temperatures everywhere several hundred degrees higher than the measured values. Since the specific heat is expected to have a direct and important effect on the observed temperatures, it is reasonable to consider the possibility that C_v is underestimated in the calculation.

At the temperatures considered in this work, the electronic contribution to the heat capacity is assumed negligible, and the molecular vibration contribution may be approximated with a value between $3R$ and the

monatomic ideal gas value of $1.5R$ per mol of atoms. The C_v value of Gurtman *et al.* is equivalent to $2.35R$ per mol of atoms, whereas the curve through the data in Fig. 5 shows that a very good agreement with experiment is obtained by simply assuming a constant $C_v = 2.9R$ per mol of atoms or $8.7R$ per mol of H_2O molecules. This value is in reasonable agreement with the results of Ree in the following paper, who calculates C_v as a function of T and V along the Hugoniot.⁷

ACKNOWLEDGMENTS

We wish to thank R. J. Trainor and M. B. Boslough for providing us with the results of their measurements of the spectral losses at the turning mirror and for several helpful discussions about the analysis of the data. We wish to acknowledge D. E. Bakker, C. D. Wozynski, H. R. Martinez, and J. Chmielewski for their assistance in firing the Lawrence Livermore National Laboratory two-stage, light-gas gun.

- ¹S. B. Kormer, *Sov. Phys. Usp.* **11**, 229 (1968).
- ²A. C. Mitchell and W. J. Nellis, *J. Chem. Phys.* **76**, 6273 (1982).
- ³M. H. Rice and J. M. Walsh, *J. Chem. Phys.* **26**, 824 (1957).
- ⁴G. A. Gurtman, J. W. Kirsch, and C. R. Hastings, *J. Appl. Phys.* **42**, 851 (1971).
- ⁵M. Cowperthwaite and R. Shaw, *J. Chem. Phys.* **53**, 555 (1970).
- ⁶M. Ross and F. H. Ree, *J. Chem. Phys.* **73**, 6146 (1980).
- ⁷F. H. Ree, *J. Chem. Phys.* **76**, 6287 (1982).
- ⁸V. Y. Klimenko and A. N. Dremin, in *Detonatsiya, Chernogolovka*, edited by O. N. Breusov *et al.* (Akad. Nauk., Moscow, 1978), p. 79.
- ⁹W. G. Hoover, *Phys. Rev. Lett.* **42**, 1531 (1979).
- ¹⁰G. A. Lyzenga and T. J. Ahrens, *Rev. Sci. Instrum.* **50**, 1421 (1979).
- ¹¹A. C. Mitchell and W. J. Nellis, *Rev. Sci. Instrum.* **52**, 347 (1981).
- ¹²S. D. Hamann, in *Modern Aspects of Electrochemistry*, edited by B. E. Conway and J. O'M. Bockris (Plenum, New York, 1974), Vol. 9, p. 126.
- ¹³Reference to a company or product name does not imply approval or recommendation of the product by the University of California or the U. S. Department of Energy to the exclusion of others that may be suitable.
- ¹⁴G. A. Lyzenga and T. J. Ahrens, *Geophys. Res. Lett.* **7**, 141 (1980).
- ¹⁵R. A. Graham and W. P. Brooks, *J. Phys. Chem. Solids* **32**, 2311 (1971).
- ¹⁶R. J. Trainor and M. B. Boslough (private communication, 1981).
- ¹⁷L. V. Altshuler, K. K. Krupnikov, B. N. Ledenev, V. I. Zhuchikhin, and M. I. Brazhnik, *Sov. Phys. JETP* **7**, 606 (1958).
- ¹⁸A. C. Mitchell and W. J. Nellis, *J. Appl. Phys.* **52**, 3363 (1981).
- ¹⁹W. J. Nellis and A. C. Mitchell, *J. Chem. Phys.* **73**, 6137 (1980).